ZaCAD Positively Regulates Chinese pepper (Zanthoxylum armatum DC.) Resistance to Rust

Shan Han
Sichuan Agricultural University
Xiu Xu
Sichuan Agricultural University
Yingming Lai
Sichuan Agricultural University
Hui Cui
Sichuan Agricultural University
Tianhui Zhu
zhuth1227@126.com

Sichuan Agricultural University

Research Article

Keywords: Chinese pepper, Zanthoxylum armatum, Coleosporium zanthoxyli, ZaCAD, RNAi, resistance gene, Y2H

Posted Date: July 22nd, 2025

DOI: https://doi.org/10.21203/rs.3.rs-7049914/v1

Additional Declarations: No competing interests reported.

Abstract

Chinese pepper rust, mainly caused by a living saprophytic fungus *Coleosporium zanthoxyli*, can seriously reduce the yield and quality of Chinese pepper. The complex mechanism underlying Chinese pepper resistance to rust remains largely unknown. In our previous study, we performed a tranomic and metabolomics analysis of leaves of resistant and susceptible Chinese pepper varieties in response to *C. zanthoxyli*, and found a gene related to lignin synthesis in *Z. armatum*, namely cinnamyl alcohol dehydrogenase *(ZaCAD)*. RNAi and overexpression vectors were constructed through in vitro recombination, and silencing and overexpression transformants of both were obtained through Agrobacterium mediated transformation. The results from Real time fluorescence quantitative PCR (qRT-PCR) demonstrated that knocking down *ZaCAD* led to a marked decrease in both lignin and total flavonoid levels in *Z. armatum*. Conversely, its overexpression resulted in a heightened accumulation of these metabolites. This suggests that *ZaCAD* plays a crucial role in the biosynthesis of secondary metabolites in plants. In addition, six related genes of secondary metabolic pathways were selected for expression detection, which showed that the relative expression levels of *ZaCAD* and the six related genes were downregulated in silenced transgenic plants and upregulated in overexpressed transgenic plants. This further indicates that *ZaCAD* regulates the biosynthesis process of secondary metabolites by affecting the expression of secondary metabolic pathway genes. In order to verify the disease resistance level of transformants, after inoculation of pathogen spore suspension, the incidence rate and disease index of *ZaCAD*-RNAi transformants increased significantly, while the incidence rate and disease index of *ZaCAD*-overexpression transformants decreased. Subcellular localization shows that *ZaCAD* is located in the nucleus and cytoplasm. Finally, Y2H technology was used to demonstrate that *ZaCAD* interacts with *GAPDH* and *MDH*. These results strongly support that *ZaCAD* activates lignin production to positively regulate the resistance of plants against *C. zanthoxyli*.

Background

Classified within the Rutaceae family, Chinese pepper (a deciduous shrub/small tree) is commercially exploited for four primary purposes: therapeutic applications, human consumption, oil production, and flavor extraction, as evidenced by numerous studies [1–5]. It has an extremely high economic and ecological value and is an important economic forest tree species native to China. Currently, China extensively cultivates two major pepper species, namely *Zanthoxylum bungeanum* Maxim (red pepper) and *Zanthoxylum armatum* DC (green pepper). According to Feng et al. [6], these crops occupy over 1.6 million hectares of farmland and generate annual revenues exceeding $2 billion USD. However, losses due to disease have been increasing annually with the rapid development of the Chinese pepper industry [7, 8]. Among them, rust is an important fungal disease endangering Chinese pepper production [9]. Rust disease can cause the leaves of Chinese pepper to drop early, which greatly affects nutrient accumulation after the disease occurs. This leads to the consumption of a large amount of nutrients for leaf regeneration, which directly affects the yield and quality of Chinese pepper in the following year [10–11]. Today, two pepper species, namely *Zanthoxylum bungeanum* Maxim (red pepper) and *Zanthoxylum armatum* DC (green pepper), are widely cultivated in China, with a planting area of more than 1.6 million

ha and an economic value of more than USD 2 billion [6]. At present, the main rust control strategies are the use of chemical pesticides and resistant varieties [12, 13]. While chemical pesticides offer certain benefits, their excessive application can lead to issues such as pesticide residues, resistance among pathogens, and a resurgence of pests [14, 15]. A more effective approach to managing plant diseases involves the cultivation and use of disease-resistant varieties [16]. Nonetheless, there is a notable absence of comprehensive research on rust resistance in *Z. armatum*, resulting in a significant gap in our understanding of rust resistance within this species.

As a phenolic macromolecule, lignin forms a structurally intricate component within the secondary walls of vascular plant cells. It plays a key role in plant growth and development and is closely combined with cellulose and hemicellulose to form the secondary cell walls [17, 18], providing mechanical strength for plants. Lignin serves a dual purpose in plants, aiding in both growth and development as well as in the plant's response to both biotic and abiotic stresses [19, 20]. Lignin accumulation was significantly elevated in the basal stem sections of *Eucalyptus urograndis* and the apical stem regions of *Eucalyptus globulus* under water deficit. This modification reduces transpirational water loss from cell walls, contributing to osmotic equilibrium and membrane defense [21]. Rice plants with upregulated OsAAE3 (a 4CL gene) exhibit reduced lignin content and weakened resistance against blast disease [22]. This gene is likely involved in the biosynthesis of lignin and other phenylpropanoid metabolites, as well as in regulating programmed cell death. In cotton, the dirigent-like gene (DIR) is significant for lignin deposition, and overexpressing *GhDIR1* markedly enhances lignification and boosts resistance to *Verticillium dahliae* in transgenic plants [23]. When plants face pathogen attacks, the host's lignin accumulation serves as a primary defense mechanism, hindering the spread of pathogens and limiting the ability of fungal enzymes and toxins to penetrate the plant cell walls. Compounds related to lignin can impair fungi's capacity to infect hosts and inhibit the reproduction and dissemination of pathogens [24]. Lignin is synthesized through the phenylpropanoid metabolic pathway, starting from the deamination reaction of amino acid phenylalanine, and finally oxidative polymerization into p-hydroxyphenol (H), guaiacol (G), syringyl (S) three lignin monomers. Plants are rich in flavonoids, which also originate from the phenylpropanoid pathway. After deamination reaction, O-methylation, and reduction reaction, 4-coumaroyl-CoA is produced and then catalyzed by intermediate enzymes, including *flavanone-3-hydroxylase* (*F3H*), *chalcone isomerase* (*CHI*), and *flavonol synthase* (*FLS*). Various flavonoids are produced under the action of *chalcone synthase* (*CHS*) [25, 26]. Flavonoids have antioxidant properties and may defend against certain diseases [27]. Similar to lignin, flavonoids are indispensable substances in plant growth and development and are also natural barriers for plants to cope with biotic and abiotic stresses [28, 29]. The heightened expression of *NtHY5* in tobacco leads to an upsurge in the activity of genes linked to phenylpropanoid pathways, which play a crucial role in regulating flavonoid biosynthesis and bolstering the plant's resilience against salt stress [30]. Furthermore, treating tangelo Nova fruits with 6-benzylaminopurine results in a notable increase in isoflavonoid levels, ultimately boosting the fruit's resistance to pathogenic fungal attacks by 60% [31].

In recent years, genetic engineering methods have developed rapidly. Genetic engineering has been successfully used to silence and overexpress genes involved in lignin and flavonoids biosynthesis,

affecting the composition and content of lignin and flavonoids in plants [32]. The main enzymes involved in lignin and flavonoids biosynthesis include *PAL*, *C4H, 4CL*, *F3H*, *cinnamoyl-CoA reductase (CCR), hydroxycinnamoyl (HCT)*, *coumaric acid 3-hydroxylase (C3H), caffeic acid-hydroxyferulic acid O-methyltransferase (COMT), caffeoyl-CoA O-methyltransferase (CCOAOMT), and cinnamyl alcohol dehydrogenase (CAD)*. Reddy obtained transgenic alfalfa by targeting the antisense downregulation of *C4H, C3H*, and *F5H*, and the transgenic line had greatly reduced lignin content [33]. Lignin is rich in p-hydroxyphenyl (H) units or guaiacol (G) units, and the S unit is reduced. Under the same genetic background, the downregulation of targeted *COMT* resulted in a significant decrease in S/G in alfalfa, while the downregulation of *CCOAOMT* reduced G lignin but not the S lignin. Nakashima obtained transgenic alfalfa lines with downregulated *4CL, CCR* and *CAD* [34]. Among them, the overall lignin content of *4CL* transgenic lines decreased by 6.6%, and the S: G ratio decreased by 0.03. Staining of the S lignin in the *CCR* and *CAD* transgenic lines was markedly significantly reduced compared to the control lines. This suggests that the antisense regulation of genes associated with lignin biosynthesis can lead to alterations in both the quantity and composition of lignin.

RNA silencing is an evolutionarily conserved sequence-specific mechanism that regulates gene expression by knocking out (or inhibiting) gene activity at the transcriptional or post-transcriptional level to verify gene function. To construct an induced silencing transgenic construct, the expression of specific genes must be inhibited to transform the target organism. The commonly used construct is composed of inverted repeat sequences homologous to the target gene, which produces double-stranded RNA that effectively induces silencing. dsRNA is effectively recognized by Dicer and cleaved into small interfering RNA (siRNA), silencing the target gene [35–38].

The *cinnamyl alcohol dehydrogenase (CAD)* gene, a key enzyme in lignin biosynthesis and the last enzyme for the synthesis of H-, G-, and S-lignin units, was first reported in 1992 [39]. The function of this gene has been studied in a variety of plant species, including Arabidopsis, tobacco, wheat, rice and poplar [39–43]. *CAD* belongs to the medium-chain dehydrogenase/reductase (MDR) family, which catalyzes the direct conversion of cinnamaldehyde to cinnamyl alcohol, and is encoded by a multi-gene family in higher plants [44]. Some of them are essential for lignin biosynthesis, which affects plant growth and development, while others function in adaptation to environmental stress [45, 46]. Molecular genetic studies have identified *AtCAD4* and *AtCAD5* as key genes responsible for generating G/S lignin building blocks [47]. *AtCAD7* and *AtCAD8* are induced by cruciferous bacterial leaf spot [40, 48, 49], and *AtCAD7* results in the loss of lignin biosynthesis activity and is a negative regulator of plant immunity induced by Phytophthora infection [50]. In addition, *CAD* transcripts expression differs among organs. For example, Populus tomentosa *CAD1 (PtoCAD1)* is highly expressed in buds, roots, xylem and phloem, with the highest expression in roots. *PtoCAD3, PtoCAD6* and *PtoCAD9* are differentially expressed among tissues [51]. *EgCAD1* and *EgCAD2* show different expression profiles, and the expression level of *EgCAD1* differs organs in the oil palm. The expression level of *EgCAD1* is the highest in the primary roots, followed by the coleoptile and young root tissues. There is low transcription in immature fruit and young leaves and no expression in peel tissues. By contrast, *EgCAD2* is highly expressed in all organs [52].

Although *CAD* has been found to be involved in the regulation of lignin and total flavonoid biosynthesis in other species, to date, no functional studies of *CAD* have been reported in *Z. armatum.* In a previous experiment, *ZaCAD* was screened from the transcriptome data during the development of Youkang and Tengjiao and highly expressed in the stem. Combined with phylogenetic analysis and homologous gene analysis of this gene and other species regulating lignin and total flavonoid synthesis, *ZaCAD* was speculated to be related to lignin and total flavonoid accumulation. Therefore, the hypothesis is proposed that "*ZaCAD* can promote the accumulation of lignin and total flavonoids, participate in regulating secondary metabolic pathways to resist the invasion of *C. zanthoxyli*". This research investigated the traits, subcellular distribution, and expression patterns of *ZaCAD*, with its functions being validated through RNA interference and overexpression in both callus and plant tissues. Additionally, proteins that interact with *ZaCAD* were identified. These findings will enhance our comprehension of the transcriptional regulatory mechanisms through which *ZaCAD* influences lignin and total flavonoid metabolism in *Z. armatum*. The aim is to elucidate the transcriptional mechanism of *ZaCAD* in regulating lignin and total flavonoid biosynthesis, providing theoretical background and technical support for the functional research of resistance genes in *Z. armatum*, and thus providing practical significance for genetic breeding.

Methods

Plant materials and microbial strains

Z. armatum seedlings (2 years old) from Hongya County, Sichuan (33°59'N, 106°39'E), were grown in Sichuan Agricultural University's greenhouse for transient transformation. Newly developed roots, stems, and leaves were sampled in triplicate. All collected tissues were flash-frozen and maintained at -80°C for future RNA extraction procedures. Pathogenic urediospores were collected from diseased *Z. armatum* leaves with clean surgical blades. After drying for 1 week, they were stored in the forest protection laboratory at -20°C and − 80°C. For subcellular localization studies, *Nicotiana benthamiana* plants were cultivated in potted soil under controlled conditions (25°C, 12 h light/12 h dark). Fresh tender leaves were collected to induce callus on MS medium for genetic transformation experiments.

CAD cloning

The CDS of *ZaCAD* was based on the sequence Cluster-20196.18748 in the *Z. armatum* transcriptome database (this sequence was screened in our previous transcriptome data analysis), and the gene was cloned from *Z. armatum* using specific primers *CAD-F/R* (Supplementary Table S1). Subsequently, the amplified product was recovered and cloned into the pEASY-T5 Zero Cloning Vector linearized vector. The correct recombinant vector extraction plasmid was stored at -20°C, and the bacterial solution was stored at -80°C.

qPCR (Real-time fluorescence quantitative PCR) analysis

We employed a standardized molecular biology workflow comprising RNA extraction, cDNA synthesis using reverse transcriptase, and quantitative PCR analysis for all *Z. armatum* samples. The β-actin gene was used as an internal reference gene for relative gene expression. The primers involved are listed in S1. Each treatment group was subjected to three qPCRs, and the average value was calculated. The analysis data were calculated using the $2^{-\Delta\Delta Ct}$ method.

The ZaCAD gene silencing in Z. armatum

The forward fragment, reverse fragment and intron fragment of *CAD* were inserted into the *KpnI* restriction site of the plant binary expression vector pCAMBIA1301-35SN. The recombinant plasmid *CAD*-pCAMBIA1301-35SN and the blank vector pCAMBIA1301-35SN were transformed into *Agrobacterium* strain GV3101, respectively. Then according to Purohit and other methods to induce callus and co-culture transformation, the Chinese pepper was instantaneously transformed according to the method of Zhou [53, 54], with each treatment being repeated three times and repeated after 3 days. After 5 days, the leaves and callus were collected and divided into 2 parts, which were stored at -80°C for DNA and RNA extraction, and the expression of target genes and related genes was detected.

Overexpression of the ZaCAD gene in Z. armatum

The complete *ZaCAD* coding sequence was PCR-amplified with gene-specific primers (see Supplementary Table S1) and subsequently cloned into the multiple cloning site of BG Plant-Express vector, where its expression was driven by the CaMV 35S promoter. Recombinant plasmids *ZaCAD-BG* Plant-Express MCS and BG Plant-Express MCS were transformed into Agrobacterium strain GV3101. Then, the single colony was selected for propagation, and the bacteria were collected by centrifugation (6,000×g, 10 min), and the bacteria were resuspended with MS heavy suspension. Finally, the bacteria were co-cultured with callus for transformation. The instantaneous transformation of *Z. armatum* was performed as mentioned above.

Identification of positive callus and positive plants

Primers Hyg501-F/R and Hyg359-F/R (Supplementary Table S1) were used for PCR amplification of the *hygromycin resistance* gene. Primers Kan270-F/R and Kan300-F/R were used for PCR amplification of the *Kan* gene. Agrobacterium was used as a positive control and sterilized ddH2O was used as a negative control to screen positive transformed leaves. Each sample had 10 biological replicates, and the obtained amplification products were sent to the company for sequencing. The successfully transformed transgenic *Z. armatum* were used for the next experiment. The positive calli of *Z. armatum* were screened with the same primers.

Pathogen inoculation and disease resistance detection

The urediospores were removed from − 20°C and activated on water agar plates to prepare a 1×10^6 spores/mL spore suspension for use. The leaf surface was washed with water (mixed with Tween 20),

and the spore suspension was sprayed onto the leaves. The inoculated leaves were maintained under moist conditions for 12 h, with disease parameters assessed 20 days later.

Disease classification was rated on a 0–4 scale, as follows: 0, leaves without urediniospore (or teleutospore) heap; 1, urediniospore (or teleutospore) accumulation accounts for about 1/10 of the leaf area; 2, urediniospore (or teleutospore) accumulation accounts for about 1/10 − 1/3 of the leaf area; 3, urediniospore (or teleutospore) accumulation accounts for about 1/3 − 1/2 of the leaf area; 4, urediniospore (or teleutospore) accumulation accounts for more than 1/2 of the leaf area.

Incidence rate I = D/T × 100% (where D represents diseased leaves, T is the total number of surveyed leaves).

Disease index = ∑ (disease level × the number of diseased plants) / (highest disease level × total number of investigated plants) × 100.

Total lignin content and total flavonoid content

Lignin was determined by the acetylation method using treated *ZaCAD*-RNAi and *ZaCAD*-overexpression plants and wild-type branches as materials. Tissue samples were oven-dried (80°C) to constant weight, ground into powder, and sieved (40 mesh) for further use, take 2 mg of sieved powder tissue, add 1.5 mL of 80% ethanol, vortex and shake well, water bath at 50℃ for 20 min, take out running water for cooling, centrifuge (12,000×g, 10 min), discard the supernatant, leave the precipitate, dry the precipitate at 95 ℃ for later use. Operate according to the instructions of the Suzhou Gree Bio Lignin Content Extraction Kit.

Lignin (mg / g) = 0.084 × (ΔA + 0.0029) ÷ W × 4, where V1 is the total volume after constant volume; W is the sample weight; and 4 is the dilution multiple of the supernatant when detected in the cuvette.

Under alkaline conditions containing nitrite, flavonoids undergo complexation with aluminum ions to generate a red-colored product exhibiting maximum absorbance at 510 nm. This chromogenic reaction forms the basis for quantifying total flavonoids via the NaNO2-Al(NO3)3-NaOH colorimetric assay. Using *ZaCCoAOMT*-RNAi, *ZaCAD*-RNAi, *ZaCCoAOMT*-overexpression, *ZaCAD*-overexpression treated strains, and wild-type as materials, the samples were incubated at 105°C for 3 min, then dried at 60°C to constant weight, crushed, and sieved through a 40 mesh sieve to obtain dried samples. Dried samples (30 mg) were homogenized in 1.5 mL of aqueous ethanol solution (60% concentration) for subsequent analysis. Following a 120-min thermal shaking extraction at 60°C, the samples were processed by refrigerated centrifugation (12,000×g, 10 min) to yield the analytical supernatant. Subsequently, the operation was carried out according to the instructions of the Suzhou Greasy Biological Total Flavonoid Content Extraction Kit.

Total flavonoid content (mg / g) = 0.4 × (ΔA + 0.0001) ÷ W × V × D, where V1 is the sample volume in the reaction; W is the sample weight; V is the volume of the extract; and D is the dilution factor.

Analysis of related gene expression

ZaCAD was analyzed using the STRING functional protein interaction database and then analyzed based on the annotation information for *Z. armatum* transcriptome data. Based on the qPCR detection data of related genes in the early stage, six related proteins were screened out: *4-coumaric acid coenzyme A ligase, hydroxycinnamoyl transferase, flavanone 3-hydroxylase, flavonoid 3-monooxygenase, coumaric acid-3-hydroxylase, and cinnamic acid 4-hydroxylase*. Wild-type cDNA was used as the control, and the β-actin plant housekeeping gene was used as the internal reference gene. The qPCR primers (Supplementary Table S1) of the six interacting proteins were predicted using design software, and fluorescence quantitative measurements were conducted following the experimental protocol detailed in 2.3 of the Materials and Methods..

ZaCAD Protein Localization Patterns in Plant Cells

The coding sequence (CDS) of *ZaCAD* was cloned into the pSuper1300-GFP vector between the *KpnI* and *XbaI* sites to obtain the *ZaCAD*-pSuper1300-GFP construct and transformed into *Agrobacterium* strain GV3101. *Nicotiana benthamiana* was infected with recombinant Agrobacterium, in which GV3101 carried the recombinant vector. The tobacco was observed under a laser confocal microscope 48–72 h after injection (FV3000, Olympus, Tokyo, Japan).

Yeast two-hybrid experiment

The Y2H (yeast two-hybrid) screening was performed with ZaCAD as bait (pGBKT7-DBD fusion) and candidate proteins as prey (pGADT7-AD fusions), using the manufacturer's protocol (GAL4 system, Cloolaber). The successfully constructed bait plasmid and prey plasmid were simultaneously transferred into yeast cells and plated on X-α-Gal solid medium. Selected single colonies were propagated in SD/-Trp/-Leu liquid medium until achieving visible cloudiness. A sterile ddH_2O was used to serially dilute the bacterial solution 10^{-2},10^{-3}, and 10^{-4} times. The undiluted bacterial solution and the serially diluted bacterial solution were taken to the second deficiency containing X-α-Gal solid medium, the third deficiency containing X-α-Gal solid medium, and the fourth deficiency containing X-α-Gal and AbA solid medium and cultured at 28°C under dark conditions. The growth state of the colony was observed to determine the interaction between the proteins.

Statistical analysis

The data of gene expression, related gene expression, incidence, disease index, total lignin content and total flavonoid content were plotted by GraphPad Prism software. The differences among treatments were statistically evaluated using Pearson's correlation analysis, with all experimental data presented as mean values ± SE (n = 3).

Results

Cloning and sequence analysis of ZaCAD

Total RNA was extracted from the leaves of *Z. armatum*, and full-length cDNA was obtained by reverse transcription. The full-length *ZaCAD* was 1074 bp, which encoded a 39.0 kDa protein containing 357 amino acids. *ZaCAD* genes were clustered with *ZaCAD* homologous sequences of Rutaceae plants (Fig. 1A) according to phylogenetic analysis. Multiple sequence alignment revealed 91.78% similarity between the target protein and its orthologs from related species (Fig. 1B). Conserved domain prediction showed that the protein contained a structure with a cinnamyl alcohol dehydrogenase function (Fig. 1C, D). A total of 22 conserved motifs were predicted by MEME, and protein homology modeling showed that closest match was to *Arabidopsis* cinnamyl alcohol dehydrogenase with four non-covalent zinc ions, indicating that the protein is cinnamyl alcohol dehydrogenase (CAD) (Fig. 1E).

ZaCAD Localization Patterns and Tissue-Specific Expression

qPCR was used to detect the expression profile of *ZaCAD* in different organs. *ZaCAD* was highly expressed in the stem, but there was low transcription in the leaves and no expression in the roots (Fig. 2A). To predict the potential role of genes involved in lignin biosynthesis in the phenylpropanoid metabolism pathway, we analyzed the differences in genes including *4CL, HCT, F3H, F3M, C3H, C4H, PAL, F35H*, and *CCOAOMT* in the Youkang and Tengjiao varieties (Fig. 2B). Compared to Tengjiao, *HCT, PAL, C4H, F3M, F3H*, and *CCOAOMT* genes were significantly upregulated. Except for PAL, the other five genes were highly upregulated, while *C3H, 4CL*, and *F35H* genes were not significantly upregulated compared to the control group. This may be due to sample size, template concentration, and experimental errors.

CAD localization was assessed using Agrobacterium-mediated transient expression in tobacco epidermis.CAD-pSuper1300-GFP fluorescence patterns showed significant overlap with nuclear indicators while remaining separate from membrane markers, indicating simultaneous presence in nucleus and cytoplasm (Fig. 2C).

Instantaneous ZaCAD overexpression promotes lignin and total flavonoid accumulation in Z. armatum

ZaCAD was transiently overexpressed in Sichuan pepper leaves to investigate their potential functions in lignin biosynthesis. PCR amplification was performed using the kan fragment on the BG Plant Express MCS plasmid to screen and identify positive strains (Fig. 3A). Quantitative RT-PCR analysis revealed a marked upregulation of *ZaCAD* gene expression in treated leaves compared to untreated controls (**$p < 0.01$, Fig. 3B). Lignin and flavonoid content determination showed that transient *ZaCAD* overexpression significantly promoted lignin and total flavonoid accumulation in *Z. armatum* (Fig. 3C, D). qPCR analysis showed that most structural genes related to the phenylpropanoid pathway (*HCT, F3H, F3M, C3H, C4H*, and *4CL*) were upregulated compared with the control group (Fig. 3E). These results indicate that *ZaCAD* positively regulates lignin and flavonoid accumulation in *Z. armatum*.

Agrobacterium-mediated CAD silencing reduces the lignin and total flavonoid content in Z. armatum

To further validate the functional role of *ZaCAD*, RNAi gene silencing technology was used to inhibit *ZaCAD* expression in *Z. armatum*. PCR amplification was performed using the hygromycin fragment on the pCAMBIA1301-35SN plasmid to screen and identify positive transformation strains (Fig. 4A). Spraying the leaves with Agrobacterium strain GV3101 containing *ZaCAD*-RNAi showed a significant decrease in *ZaCAD* expression (Fig. 4B). Compared with the wild type, the total flavonoid and lignin contents of *CAD*-silenced plants were significantly reduced (Fig. 4C, D). qPCR results indicated suppressed expression of critical enzymes in the phenylpropanoid pathway, including HCT, F3H, F3M, C3H, C4H, and 4CL, which coordinate lignin and flavonoid formation (Fig. 4E). These results confirm that *ZaCAD* positively regulates lignin and flavonoid accumulation in *Z. armatum*.

Stable overexpression and silencing of ZaCAD and related gene expression analysis

The *ZaCAD* gene was overexpressed and silenced in *Z. armatum* callus tissue (Fig. 5) to determine whether it regulated the expression of phenylpropanoid-related genes. Compared with W, the transcription levels in *ZaCAD*-silenced plants decreased (Fig. 6A); the relative expression level in plants overexpressing *ZaCAD* increased (Fig. 6C). The expression levels of lignin and total flavonoid synthesis genes (Fig. 6B), including *4CL, HCT, F3M, F3H, C4H*, and *C3H*, were downregulated in the silenced system but upregulated in overexpression lines (Fig. 6D). The results indicate that ZaCAD is a positive regulatory factor for lignin and flavonoid accumulation in *Z. armatum*.

Detection of disease resistance level

After inoculating control and experimental *Z. armatum* plants with fungal spores, disease progression was evaluated after 20 days, with the incidence and disease index (Table 1). The *CAD*-overexpression treatment group had the lowest incidence rate and disease index (22.7 and 5.7, respectively). The overexpression lines demonstrated modest improvements in disease resistance parameters, with mean incidence rates of 22.7 ± 0.01% versus 34.0 ± 0.05% in controls, and disease index of 5.7 ± 0.17 versus 14.2 ± 3.66, respectively (n = 3 biological replicates, $p > 0.05$). Among all experimental groups, the *CAD*-RNAi treatment showed maximal disease susceptibility, demonstrating 67.3% incidence and a disease index of 57.2.. The incidence rate and disease index were significantly higher in *Z. armatum* after expression interference of disease candidate genes than in the control group.Twenty days after inoculation, the differences in symptoms between the control group and the treatment group were significant (Fig. 7). After inoculation with the spore suspension, the control group showed five clusters on the back of the leaves, with a slight expansion of the clusters. In the *CAD*-overexpression treatment group, only one cluster appeared, and the symptoms were significantly reduced compared with the control group. The *CAD*-RNAi treatment group had the most severe disease symptoms, with seven clusters appearing and expanding toward the surrounding areas.

Table 1
Statistics of incidence rate and Disease Index

Varieties	Incidence(%)	Disease Index
CK	34.0 ± 0.05	20.2 ± 3.66
CAD-RNAi	67.3 ± 0.11*	57.2 ± 13.13*
CAD-overexpression	22.7 ± 0.01	5.7 ± 0.17

Note: The data are the mean value ± standard error of the three biological replicates, * indicates that the data of the same column are significantly different between different treatments by independent sample t test ($P < 0.05$).

ZaCAD can bind to ZaGAPDH and ZaMDH and activate the expression level

The amplified *ZaCAD* gene fragment was homologous recombined with the linearized vector pGBKT7 to obtain the recombinant plasmid pGBKT7-*ZaCAD*. After colony PCR detection, it matched the theoretical length and was validated by sequencing. Sequencing the PCR product to confirm that it is a positive clone.

The plasmid pGBKT7 Lam and pGADT7-T control vectors were used as negative controls, while the plasmid pGBKT7-53 and pGADT7-T control vectors were used as positive controls. The pGBKT7-53 and pGADT7-T control vectors showed clone growth in DDO (SD/-Trp/-Leu/X-α-Gal), TDO (SD-Trp/-Leu/-His/X-α-Gal), and QDO (SD-Trp/-Leu/-His/-Ade/X-α-Gal/AbA) media, and the positive control experiment was successful. The pGBKT7 Lam and pGADT7-T control vectors were grown on DDO medium, but no clone growth was observed on TDO or QDO medium. The negative control experiment was successful. The BD gene pGBKT7-*CAD* + pGADT7 grew on DDO, indicating that the pGBKT7-*CAD* plasmid was successfully transferred into the yeast strain, with slight growth on TDO and no growth on QDO medium. This showed that pGBKT7-*CAD* had slight self-activation activity in Y2H golden yeast strains and could be used for screening experiments.

After co-culturing the yeast library with the bait expression vector, the cultured bacterial liquid was observed microscopically. Under a 40-fold microscope, a Mickey head yeast conjugate with characteristic morphology was observed, indicating that the bait protein was successfully hybridized with the protein in the library. About 80 positive clones were grown in the selective TDO medium. The colonies on the primary screening plate were selected and transferred again to QDO/AbA/X-α-Gal screening plates. For further screening, 41 clones were obtained, of which 3 did not grow and the rest grew normally and became blue; thus, 38 positive clones were obtained (Fig. 9). The pGADT7 universal primer was used to amplify the colony PCR to detect the inserted fragment in the blue clone, and the PCR product was sequenced. The 38 positive clones interacting with *ZaCAD* were subjected to BLAST alignment, and the positive clones that could not be compared were removed. A total of 11 sequences were screened, and 11 positive clones were screened for gene annotation: AP-4 complex subunit sigma, 50S ribosomal protein L18, cytokinin riboside 5'-monophosphate, tripeptidyl-peptidase 2, auxin efflux

carrier component 3, glyceraldehyde-3-phosphate dehydrogenase A, chloroplast envelope quinone oxidoreductase homolog, subtilisin-like protease SBT1.5, malate dehydrogenase, plastid-lipid-associated protein, and serine/arginine-rich splicing factor SR34A.

The screened plasmids were co-transformed with pGBKT7-*ZaCAD* into the Y2H Gold yeast strain for one-to-one hybridization experiments, and spot plate verification was performed. There were negative control, positive control, and empty plasmid control groups. pGBKT7-*ZaCAD* + pGADT7-*CcGAPDH* and pGBKT7-*ZaCAD* + pGADT7-*CcMDH* grew blue clones on QDO/X/A medium. However, pGBKT7-*ZaCAD* + pGADT7-*CcAP4S*, pGBKT7-*ZaCAD* + pGADT7-*CcRPIR*, pGBKT7-*ZaCAD* + pGADT7-*CsCR5-MP*, pGBKT7-*ZaCAD* + pGADT7-*CcTP2*, pGBKT7-*ZaCAD* + pGADT7-*CcAECC3*, pGBKT7-*ZaCAD* + pGADT7-*CsceQORH*, pGBKT7-*ZaCAD* + pGADT7-*CcSBT1.5*, and pGBKT7-*ZaCAD* + pGADT7-*CsPAP* did not grow on QDO/X/A medium (Fig. 10). This indicates that *ZaCAD* interacted with *GAPDH* and *MDH* genes but not with other genes.

Discussion

Lignin and flavonoids are natural barriers for plants to resist adversity. Understanding the formation and regulatory mechanisms of lignin and flavonoids in plant species will allow a better understanding of plant resistance mechanisms. This study identified a novel gene, *ZaCAD*, and showed that this gene is involved in regulating lignin and flavonoid formation in *Z. armatum*. Transgenic studies successfully validated its function and uncovered potential regulatory mechanisms.

In this experiment, the nucleic acid sequence of the gene of interest was highly similar to the gene annotated as *ZaCAD* in the database, and its encoded protein was highly similar to *CAD* proteins of other species (Fig. 1A), which is consistent with previous results shown by cloning *CAD* genes [41, 43]. As the final step in catalyzing lignin monomer synthesis, *CAD* plays a core role in regulating lignin biosynthesis by reducing hydroxycinnamaldehyde to corresponding alcohols [46]. Moreover, different families of *CAD* genes exhibit functional division during plant growth and development and are expressed in different tissues and stages [51, 52]. This study found that *ZaCAD* is preferentially expressed in the stems and leaves of *Z. armatum* but not in the roots (Fig. 2A), and it is significantly correlated with the lignin and flavonoid content as well as the expression level of biosynthetic genes (Fig. 2B). According to phylogenetic analysis, *ZaCAD* is closely clustered with citrus *CAD*, with a phylogenetic relationship of 99% (Fig. 1A). Multiple sequence alignment analysis showed consistency between this gene and other protein sequences, which reached 91.78% (Fig. 1B), suggesting that this gene has similar functions.

The use of RNA antisense interference technology to silence the *ZaCAD* gene in tall fescue resulted in a 30–50% reduction in *ZaCAD* activity, a 15% reduction in lignin, and a reduction in G- and S-lignin monomer content in transgenic plants [55]. The effect is similar to that in transgenic tobacco and alfalfa obtained after silencing *CAD* [56, 57]. This study also obtained similar results; that is, transient *CAD* overexpression increased the expression of this gene in transgenic lines, and the expression levels of *4CL, HCT, C3H, C4H, F3H*, and *F3M* in the phenylpropanoid pathway were also upregulated in

overexpressing lines (Fig. 3E, Fig. 6D). This result is consistent with that in transgenic macaques [58], where *AcNADS32* regulates the expression of carotenoid biosynthesis-related genes *ZEP, VDE, BCH1*, and *BCH2* to regulate the fruit ripening process. *CAD* overexpression promoted the lignin and flavonoid contents in *Z. armatum*, which is consistent with the increase in flavonoid content caused by *F3H* gene overexpression in tomato [59]. Subsequently, *Agrobacterium*-mediated *CAD*-silenced transformed strains significantly inhibited the lignin and total flavonoid contents and downregulated the *4CL, HCT, C3H, C4H, F3H*, and *F3M* genes (Fig. 4C, D, E). Similar results have also been found in transgenic tobacco, where downregulation of *C4H* expression resulted in lower transcription levels of phenylpropanoid pathway genes *PAL, 4CL, CCOAOMT*, and *CAD* compared with the control group. Following from these discoveries,, we speculate that *CAD* acts on the lignin biosynthesis pathway to regulate lignin accumulation in *Z. armatum*.

For functional characterization of CAD in lignin and flavonoid metabolism, we developed stable transgenic *Z. armatum* callus lines, including three independent overexpression and three knockdown lines. All genes related to the lignin and flavonoid biosynthesis pathways were downregulated in the callus tissues of silenced transgenic strains (Fig. 6B), while gene expression was upregulated in overexpressed strains (Fig. 6D), consistent with the results obtained in previous transient transformations.

In this study, a cDNA library was preliminarily screened using *ZaCAD* as a bait protein, and 11 proteins interacting with *ZaCAD* were screened by sequencing (Fig. 9). The proteins interacting with *ZaCAD*, namely *GAPDH* and *MDH*, were verified using a one-to-one plate of bait protein and prey protein (Fig. 10). *Glyceraldehyde 3-phosphate dehydrogenase A* (*GAPDH*) is a highly conserved glycolytic enzyme that participates in the first energy production reaction in the glycolysis pathway, catalyzing the oxidative phosphorylation of glyceraldehyde-3-phosphate to produce nicotinamide adenine dinucleotide (NADH) [60]. Malic acid dehydrogenase *(MDH)* is a common oxidoreductase that primarily catalyzes the reversible conversion of (L -) malic acid to oxaloacetate in the C4 photosynthetic pathway of plants, maintaining a dynamic balance between the two. In this study, it was demonstrated that *ZaCAD* interacts with *GAPDH* and *MDH*. *GAPDH* may affect the energy supply and metabolite synthesis of plants by regulating the activity of the glycolysis pathway, indirectly affecting the synthesis of lignin and flavonoids. *MDH* is involved in regulating various metabolic processes, such as the tricarboxylic acid cycle (TCA) and glyoxylate cycle. By regulating the activity of metabolic processes, it affects carbon metabolism in plants and accumulates precursor substances for lignin and flavonoid biosynthesis, such as phenylalanine and cinnamic acid [61]. In addition, *GAPDH* and *MDH* both participate in intracellular redox reactions, helping to maintain the balance of NAD+/NADH. *CAD*, as a key enzyme in the lignin synthesis pathway, relies on NADPH as a cofactor. Therefore, the interaction between these enzymes may affect the activity of CAD and consequently the synthesis of lignin by regulating the supply of *NADPH*. The functional studies of most *CADs* genes have shown that when plants are damaged by external environments, they synthesize lignin to cope with stress. *GAPDH* and *MDH* participate in regulating the expression of stress-related genes through their interaction with *CAD*, including genes encoding lignin and flavonoid biosynthesis pathways. And since *GAPDH* is mainly located in the

cytoplasm, while *MDH* is distributed in both the cytoplasm and mitochondria, the interaction between *CAD* and them may promote the exchange of substances and information between different organelles, which is crucial for coordinating the metabolic activities of the entire cell [62, 63]. These effects indicate that *ZaCAD* forms a complex with *GAPDH* and *MDH* to synergistically participate in various metabolic cycles such as glycolysis and TCA in *Z. armatum*, providing a prerequisite for the normal operation of the phenylpropane metabolic pathway downstream of *Z. armatum* and laying the foundation for its involvement in stress resistant branching pathways. In summary, *ZaCAD* has more precise and complex regulatory abilities in the biological functions of *Z. armatum*. These findings not only contribute to a deeper understanding of the specific mechanisms of action of *ZaCAD*, but also provide new directions for further research on its role in stress response. Future research can continue to explore the interactions between *ZaCAD* and key enzymes in other metabolic pathways to reveal its comprehensive role in plant physiological processes.

The ZaCAD gene was identified as a nuclear-localized transcription factor based on subcellular localization results (Fig. 2C). Transcription factors typically exert regulatory effects by binding to multiple genes. Our experiments confirmed interactions between ZaCAD and two proteins, GAPDH and MDH, but further research is needed to explore additional binding partners. These observations imply that ZaCAD may function both independently in transcriptional regulation and cooperatively within protein complexes to fine-tune complex metabolic pathways.

Conclusion

In summary, the present study revealed that lignin and total flavonoid biosynthesis in *Z. armatum* was regulated by changing the transcription level of the *CAD* gene. These results enrich our understanding of the transcriptional mechanism of lignin and flavonoid biosynthesis.

Declarations

Acknowledgements

Not applicable.

Authors' contributions

Shan Han: Conceptualization, Methodology, Data Curation, Writing - Review & Editing, Funding acquisition. Yingming Lai and Xiu Xu: Writing - Original Draft, Formal analysis, Investigation. Hui Cui: Validation, Resources, Data Curation. Tianhui Zhu: Writing - Review & Editing, Supervision, Project administration.

Funding

This work was financially supported by the Science and Technology Department of Sichuan Province (2024NSFSC0327).

Data availability

All data supporting this study are included in the manuscript and its Supplementary Information. Additional data are available from the corresponding author upon reasonable request.

Ethics approval and consent to participate

Not applicable.

Consent for publication

Not applicable.

Competing Interests

The authors declare no competing interests.

References

1. X. Chen, X. Jin, Y. Li, G. Chen, K. Chen, J. Kan: **Preparation and characterization of molecularly-imprinted polymers for extraction of sanshool acid amide compounds followed by their separation from pepper oil resin derived from Chinese prickly ash (*Zanthoxylum bungeanum*).** *J Sep Sci* 2018, **41**(2): 590-601.
2. E.V. Kharshiing: **Aqueous extracts of dried fruits of Zanthoxylum armatum DC., (Rutaceae) induce cellular and nuclear damage coupled with inhibition of mitotic activity in vivo**. *American Journal of Plant Sciences* 2012, **3** (11): 1646-1653.
3. K. Ryo, M. Kaneko, K. Takahashi, H. Ono, T. Ogasawara, M. Abe, I. Saito.: **Study on the salivation effect of encapsulated food products containing Sichuan pepper oil**. *Clin Exp Dent Res* 2019, **5**(1): 7-13.
4. S. Mishra, S. Joshi, M.L. Sah, D. Mishra, M. Bisht: **Biological activities of the essential oil of *Zanthoxylum armatum* DC. leaves.** *The Natural Products Journal* 2014, **4** (3): 229-232.
5. Z. Nooreen, S. Singh, D.K. Singh, S. Tandon, A. Ahmad, S. Luqman: **Characterization and evaluation of bioactive polyphenolic constituents from *Zanthoxylum armatum* DC., a traditionally used plant.** *Biomedicine & Pharmacotherapy* 2017, **89** (1): 366-375.
6. S.J. Feng, Z.S. Liu, J. Cheng, Z.H. Li, L. Tian, M. Liu, T.X. Yang, Y.L. Liu, Y.H. Liu, H. Dai, Z.J. Yang, Q. Zhang, G. Wang, J.S. Zhang, H.F. Jiang, A.Z. Wei: **Zanthoxylum-specific whole genome duplication and recent activity of transposable elements in the highly repetitive paleotetraploid Z. bungeanum genome.** *Hortic. Res* 2021, **8** (1): 205.
7. Y.F. Cao, L.F. Wang, X.Z. Wang, Z.L. Xu, Y. Li, L. Yao: **Pathogen identification of root knot nematode disease in nine leaf green and white pepper.** *Plant Protection* 2019, **45** (5): 242-246.

8. S. Han, Z.L. Zheng, S. Li, Y.G. Liu, S.L. Li, C.L. Yang, T.M. Qiao, T.T. Lin, T.H. Zhu: **Impact of Root Rot Disease of *Zanthoxylum armatum* on Rhizosphere Soil Microbes and Screening of Antagonistic Bacteria.** *Forests* 2023, **14** (1561): 1561.
9. H.D. Shin, C.H. Jeon, W.I. Choi: **First report of rust caused by *Coleosporium zanthoxyli* on *Zanthoxylum planispinum* in Korea**. *Plant Disease* 2019, 103 (2): 371-372.
10. S. Han, X. Xu, H. Yuan, S.J. Li, T.T. Lin, Y.G. Liu, S.Y. Li, T.H. Zhu: **Integrated Transcriptome and Met abolome Analysis Reveals the Molecular Mechanism of Rust Resistance in Resistant (Youkang) and Susceptive (Tengjiao) *Zanthoxylum armatum* Cultivars.** *International Journal of Molecular Sciences*. 2023, **24** (19): 14761.
11. M. Hu, M. Ye, Y. Gou: **Morphological differentiation and bud structure of bamboo leaf Sichuan pepper.** *Journal of Nuclear Agriculture* 2019, **33** (7): 1415-1422.
12. D. Deb, B.A. Engel, J. Harbor, L. Hahn, K.J. Lim, T. Zhai: **Investigating potential water quality impacts of fungicides used to combat soybean rust in indiana**. *Water Air & Soil Pollution* 2010, **207** (1-4): 273-288.
13. A. Horsfield'P, T. Wicks, D. Wilson: **Field evaluation of fungicides for the control of rust, brown rot, shot hole and scab in almonds**. Australas. *Plant Pathol* 2010, **39** (3): 112–119.
14. N.J. Hawkins, C. Bass, A. Dixon, P. Neve: **The evolutionary origins of pesticide resistance.** *Biol. Rev* 2019, **94** (1): 135-155.
15. J.H. Westwood, R. Charudattan, S.O. Duke, S.A. Fennimore, P. Marrone, D.C. Slaughter: **Weed management in 2050: Perspectives on the future of weed science.** *Weed Sci* 2018, **66** (3): 275-285.
16. N. Wang, C.L. Tang, X. Fan, M.Y He, P.F. Gan, S. Zhang, Z.Y. Hu, X.D. Wang, T. Yan, W.X. Shu, L.G. Yu, J.R. Zhao, J.N. He, L.L. Li, J.F. Wang, X.L. Huang, L.L. Huang, J.M. Zhou, Z.S. Kang, X.J. Wang: **Inactivation of a wheat protein kinase gene confers broad-spectrum resistance to rust fungi**. *Cell* 2022, **185** (16): 2961-2974(e19).
17. Z.H. Ye: **Transcriptional activation of secondary wall biosynthesis by rice and maize NAC and MYB transcription factors.** *Plant and Cell Physiology* 2011, **52** (10): 1856-1871.
18. I. Cesarino: **Structural features and regulation of lignin deposited upon biotic and abiotic stresses.** *Current opinion in biotechnology* 2019, **56** (0): 209-214.
19. J. Barros, H. Serk, I. Granlund: **The cell biology of lignification in higher plants.** *Annals of botany* 2015, **115** (7): 1053-1074.
20. R. Dean, J. Kan, Z.A. Pretorius, K.E. Hammond-Kosack, A.D. Pietro, P.D. Spanu, J.J. Rudd, M. Dickman, R Kahmann, J. Ellis: **The Top 10 fungal pathogens in molecular plant pathology.** *Mol. Plant Pathol* 2012, **13** (4): 414–430.
21. J. Moura-sobczak, U. Souza, P. Mazzafera: **Drought stress and changes in the lignin content and composition in Eucalyptus.** *BMC Proceedings* 2011, **5** (7): 103.
22. H. Liu, Z. Guo, F. Gu: **4-Coumarate-CoA Ligase-Like Gene OsAAE3 Negatively Mediates the Rice Blast Resistance. Floret Development and Lignin Biosynthesis**. *Frontiers in Plant Science* 2017, 7 (1): 2041.

23. H. Shi, Z. Liu, L. Zhu: **Overexpression of cotton (*Gossypium hirsutum*) dirigent1 gene enhances lignification that blocks the spread of Verticillium dahliae**. *Acta Biochimica et Biophysica Sinica* 2012, **44** (7): 555-564.

24. Q. Liu, L. Luo, L. Zheng: **Lignins: Biosynthesis and Biological Functions in Plants.** *International Journal of Molecular Sciences* 2018, **19** (2): 335.

25. Y. Wu, C. Zhang, Z Huang, L.L. Yu, W. Li, W. Wu: **Integrative analysis of the metabolome and transcriptome provides insights into the mechanisms of flavonoid biosynthesis in blackberry.** *Food Research International* 2022, **153** (Suppl C): 110948.

26. T. Ding, R. Zhang, H. Zhang, Z. Zhou, Z. Yan: **Identification of gene co-expression networks and key genes regulating flavonoid accumulation in apple (Malus× domestica) fruit skin.** *Plant Science* 2021, **304**: 110747.

27. L. Alvarez-Jubete, H. Wijngaard, E.K. Arendt, E. Gallagher: **Polyphenol composition and in vitro antioxidant activity of amaranth, quinoa buckwheat and wheat as affected by sprouting and baking.** *Food chemistry* 2009, **119** (2): 770-778.

28. S. B. Winkel: **Biosynthesis of flavonoids and effects of stress.** *Current opinion in plant biology* 2002, **5** (3): 218-223.

29. M. Havaux, K. Kloppstech: **The protective functions of carotenoid and flavonoid pigments against excess visible radiation at chilling temperature investigated in Arabidopsis npq and tt mutants.** *Planta* 2001, **213** (6), 953-966.

30. Deeksha Singh, Shambhavi Dwivedi, Hiteshwari Sinha, Nivedita Singh, Prabodh Kumar Trivedi: **Mutation in shoot-to-root mobile transcription factor, ELONGATED HYPOCOTYL 5, leads to low 3 nicotine levels in tobacco**. *Journal of Hazardous Materials* 2023, **465**: 133255.

31. A. Ortuno, M.C. Arcas, J.M. Botia: **Increasing Resistance against Phytophthora citrophthora in Tangelo Nova Fruits by Modulating Polymethoxyflavones Levels**. *Journal of Agricultural and Food Chemistry* 2002, **50** (10): 2836-2839.

32. S. Fornaléa, M. Capelladesa, A. Encinab, K. Wangc, S. Irara, C.e Lapierred, K. Ruele, J.P. Joseleaue, J. Berenguera, P. Puigdomènecha, J. Rigaua, D. Caparrós-Ruiza: **Altered Lignin Biosynthesis Improves Cellulosic Bioethanol Production in Transgenic Maize Plants Down-Regulated for Cinnamyl Alcohol Dehydrogenase.** *Molecular Plant* 2012,**5** (4): 817-830.

33. M.S. Reddy, F. Chen, G. Shadle, L. Jackson, H. Aljoe, R.A. Dixon: **Targeted down-regulation of cytochrome P450 enzymes for forage quality improvement in alfalfa (*Medicago sativa* L.).** *Proceedings of the National Academy of Sciences* 2005, **102** (46):16573-16578.

34. N. Jin, F. Chen, L. Jackson, G. Shadle, R.A. Dixon: **Multi-site genetic modification of monolignol biosynthesis in alfalfa (*Medicago sativa*): effects on lignin composition in specific cell types.** *New Phytologist* 2008, **179** (3): 738-750.

35. N.G. Bologna, R. Iselin, L.A. Abriata, A. Sarazin, N. Pumplin, F. Jay, T. Grentzinger, M.D. Peraro, O. Voinnet: **Nucleo-cytosolic shuttling of ARGONAUTE1 prompts a revised model of the plant microRNA pathway.** *Molecular Cell* 2018, **69** (4): 709-719.

36. J.H. Zhao, H.S. Guo: **RNA silencing: From discovery and elucidation to application and perspectives.** *Journal of Integrative Plant Biology* 2022, **64** (2): 476-498.

37. Y. Dang, Q. Yang, Z. Xue, Y. Liu: **RNA interference in fungi: pathways, functions, and applications.** *Eukaryotic cell* 2011, **10** (9): 1148-1155.

38. L. Li, S.S. Chang, L. Yi: **RNA interference pathways in filamentous fungi.** *Cellular and molecular life sciences* 2010, **67** (22): 3849-3863.

39. M. -E. Knight, C. Halpin, W. Schuch: **Identification and characterisation of cDNA clones encoding cinnamyl alcohol dehydrogenase from tobacco.** *Plant Molecular Biology* 1992, 19 (5): 793-801.

40. R. Sibout, A. Eudes, G. Mouille, B. Pollet, A. Séguin: **CINNAMYL ALCOHOL DEHYDROGENASE-C and-D are the primary genes involved in lignin biosynthesis in the floral stem of Arabidopsis.** *The Plant Cell* 2005, **17** (7):2059-2076.

41. C. Chen, J. Chang, S. Wang, J. Lu, C. Ma: **Cloning, expression analysis and molecular marker development of cinnamyl alcohol dehydrogenase gene in common wheat.** *Protoplasma* 2021, **258** (4): 881-889.

42. C. M. Tobias, E. K. Chow: **Structure of the cinnamyl-alcohol dehydrogenase gene family in rice and promoter activity of a member associated with lignification.** *Planta* 2005, **220** (5): 678-688.

43. A. Barakat, A. Bagniewska-Zadworna, A. Choi, U. Plakkat, D.S. Diloreto, Y. J. E Carlson: **The cinnamyl alcohol dehydrogenase gene family in Populus: phylogeny, organization, and expression.** *BMC plant biology* 2009, **9** (1): 26.

44. T. Zhang, F. Bao, A. Ding, Y.J. Yang, T. Cheng, J. Wang, Q. Zhang: **Comprehensive analysis of endogenous volatile compounds, transcriptome, and enzyme activity reveals PmCAD1 involved in cinnamyl alcohol synthesis in *Prunus mume*.** *Frontiers in plant science* 2022, **13**: 820742.

45. S. Jiang, X. Tian, X. Huang, J. Xin, H. Yan: **Physcomitrium patens CAD1 has distinct roles in growth and resistance to biotic stress.** *BMC Plant Biology* 2022, **22** (1): 518.

46. D. M. Guo, J.H. Ran, X.Q. Wang: **Evolution of the cinnamyl/sinapyl alcohol dehydrogenase (CAD/SAD) gene family: the emergence of real lignin is associated with the origin of bona fide CAD**. *Journal of Molecular Evolution* 2010, **71** (3): 202-218.

47. B. Youn, R. Camacho, S.G.A. Moinuddin, C. Lee, L. B. Davin,, N. G. Lewis, C.H. Kang: **Crystal structures and catalytic mechanism of the Arabidopsis cinnamyl alcohol dehydrogenases AtCAD5 and AtCAD4.** Organic & biomolecular chemistry 2006, **4** (9): 1687-1697.

48. M. Tronchet, C. Balagué, T. Kroj, L. Jouanin, D. Roby: **Cinnamyl alcohol dehydrogenases-C and D, key enzymes in lignin biosynthesis, play an essential role in disease resistance in Arabidopsis.** *Molecular plant pathology* 2010, **11** (1): 83-92.

49. S. Kiedrowski, P. Kawalleck, K. Hahlbrock: **Rapid activation of a novel plant defense gene is strictly dependent on the Arabidopsis RPM1 disease resistance locus.** *The EMBO Journal* 1992, **11** (13): 4677-4684.

50. T.T. Li, Q.H. Wang, R.R. Feng, L.C. Li, L.W. Ding, G.J. Fan: **Negative regulators of plant immunity derived from cinnamyl alcohol dehydrogenases are targeted by multiple Phytophthora Avr3a-like**

effectors. *New Phytol* 2019, **2019** (0):1.

51. N. Chao, S.X. Liu, B.M. Liu, N. Li, X.N. Jiang, Y. Gai: **Molecular cloning and functional analysis of nine cinnamyl alcohol dehydrogenase family members in Populus tomentosa.** *Planta* 2014, **240** (5): 1097-1112.
52. C.Y.L. Yusuf, N.S. Nabilah, N.AAM Taufik, I.A. Seman, M.P. Abdullah: **Genome-wide analysis of the CAD gene family reveals two bona fide CAD genes in oil palm**. *Biotech* 2022, **12** (7): 1-19.
53. S. Purohit, K. Joshi, V. Rawat, I.D. Bhatt, S.K. Nandi: **Efficient plant regeneration through callus in Zanthoxylum armatum DC: an endangered medicinal plant of the Indian Himalayan region.** *Plant Biosystems* 2020, **154** (3): 288-294.
54. R. Zhou, Y.H. Don, X. Liu, S. Feng, C.X. Wang, X.M. Ma, J.N. Liu, Q. Liang, Yan Bao, S.Y. Xu, X.Y. Lang, S.S. Gai, K.Q. Yang, H.C. Fang: **JrWRKY21 interacts with JrPTI5L to activate the expression of JrPR5L for resistance to Colletotrichum gloeosporioides in walnut.** *The Plant Journal* 2022, **111** (4): 1152-1166.
55. A.J. Saathoff, S. Gautam, E.K. Chow, B.S. Dien, C.M. Tobias, H.E. Alfredo: **Downregulation of cinnamyl-alcohol dehydrogenase in switchgrass by RNA silencing results in enhanced glucose release after cellulase treatment**. *PLoS One* 2011, **6** (1): e16416.
56. M. Chabannes, A. Barakate, C. Lapierre, J.M. Marita, J. Ralph, M. Pean, S Danoun, C. Halpin, J. Grima-Pettenati, A.A.M. Boudet: **Strong decrease in lignin content without significant alteration of plant development is induced by simultaneous down-regulation of cinnamoyl CoA reductase (CCR) and cinnamyl alcohol dehydrogenase (CAD) in tobacco plants.** *The Plant Journal* 2001, **28** (3); 257-270.
57. M. Baucher, M.A. Bernard-Vailhé, B. Chabbert, J.M. Besle, C. Opsomer, M.V. Montagu, J. Botterman: **Down-regulation of cinnamyl alcohol dehydrogenase in transgenic alfalfa (*Medicago sativa* L.) and the effect on lignin composition and digestibility.** *Plant molecular biology* 1999, **39** (3): 437-447.
58. H. Xia, Z.Y. Lin, Z.C. He, Y.Q. Guo, X.L. Liu, H.H. Deng, M.Z. Li, Y. Xie, M.F. Zhang, J. Wang, X.L. Lv, Q.X. Deng, X. Luo, Y. Tang, L.J. Lin, D. Liang: **AcMADS32 positively regulates carotenoid biosynthesis in kiwifruit by activating AcBCH1/2 expression**. *International Journal of Biological Macromolecules* 2023, **242** (part 3): 124928.
59. C. Meng, S. Zhang, Y.S. Deng, G.D. Wang, F.Y. Kong: **Overexpression of a tomato flavanone 3-hydroxylase-like protein gene improves chilling tolerance in tobacco**. *Plant Physiology and Biochemistry* 2015, **96**: 388-400.
60. M.A. Sirover: **The role of posttranslational modification in moonlighting glyceraldehyde-3-phosphate dehydrogenase structure and function.** *Amino Acids* 2021, **53** (4): 507-515.
61. J. Omini, I. Wojciechowska, A. Skirycz: **Association of the malate dehydrogenase-citrate synthase metabolon is modulated by intermediates of the Krebs tricarboxylic acid cycle.** *Scientific Reports* 2021, **11** (1): 18770.
62. J.H. Ahn, H. Seo, W. Park: **Enhanced succinic acid production by Mannheimia employing optimal malate dehydrogenase.** *Nature Communications* 2020, **11** (1): 1970.

63. M. Ranjbar, F. Khakdan, A. Ghorbani: **The variations in gene expression of GAPDH in Ocimum basilicum cultivars under drought-induced stress conditions.** *Environmental Science and Pollution Research* 2023, **30** (56): 119187-119203.

Figures

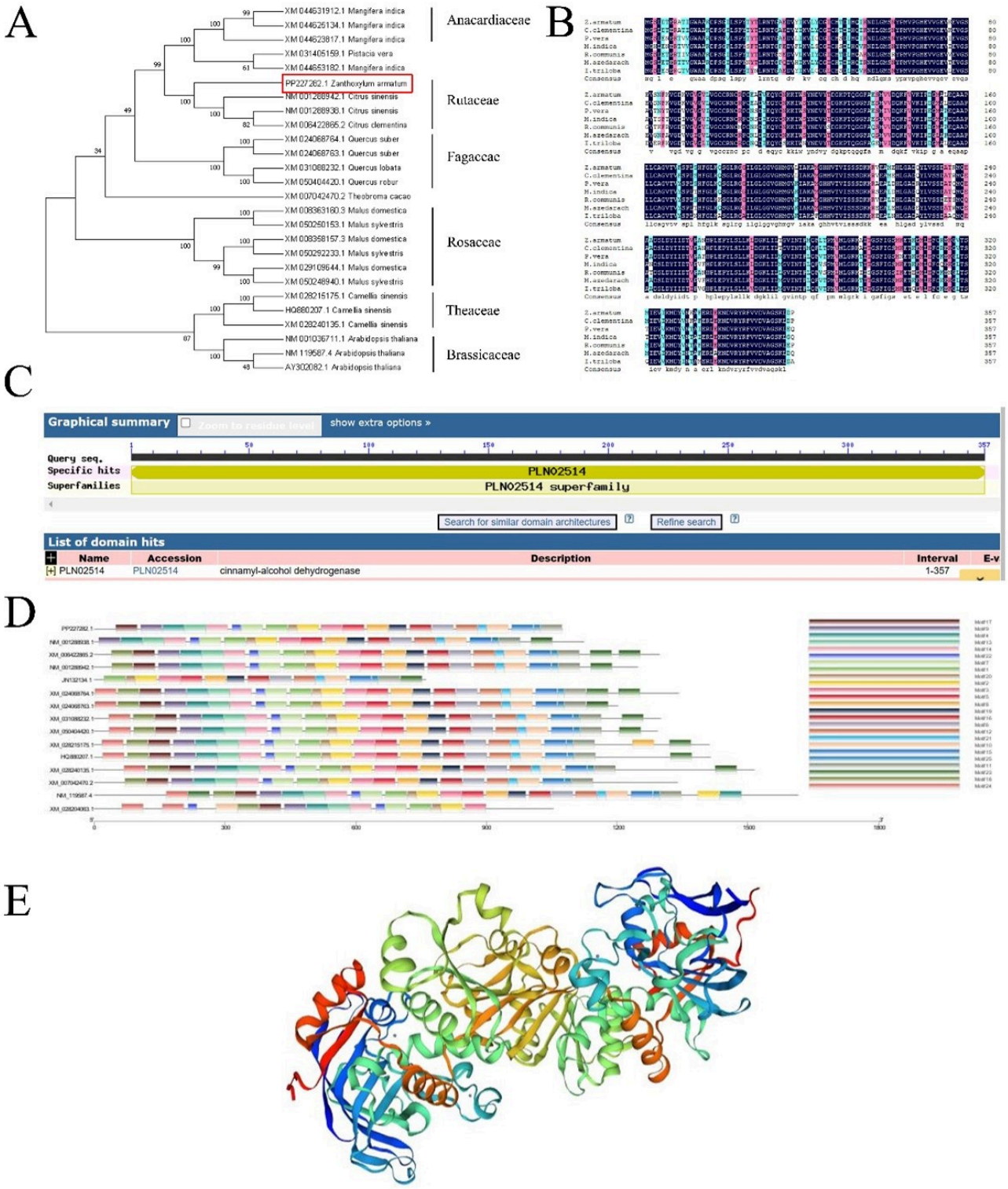

Figure 1

ZaCAD gene sequence analysis. (A) A target gene development tree based on Neighbor Jiung algorithm, with red boxes representing *ZaCAD*. (B) Multi sequence alignment between *ZaCAD* and other species *ZaCAD*. (C) Conservative domain prediction of *ZaCAD* genes. (D) Conservative motif prediction of *ZaCAD* genes. (E) *ZaCAD* encoded protein tertiary structure homology modeling.

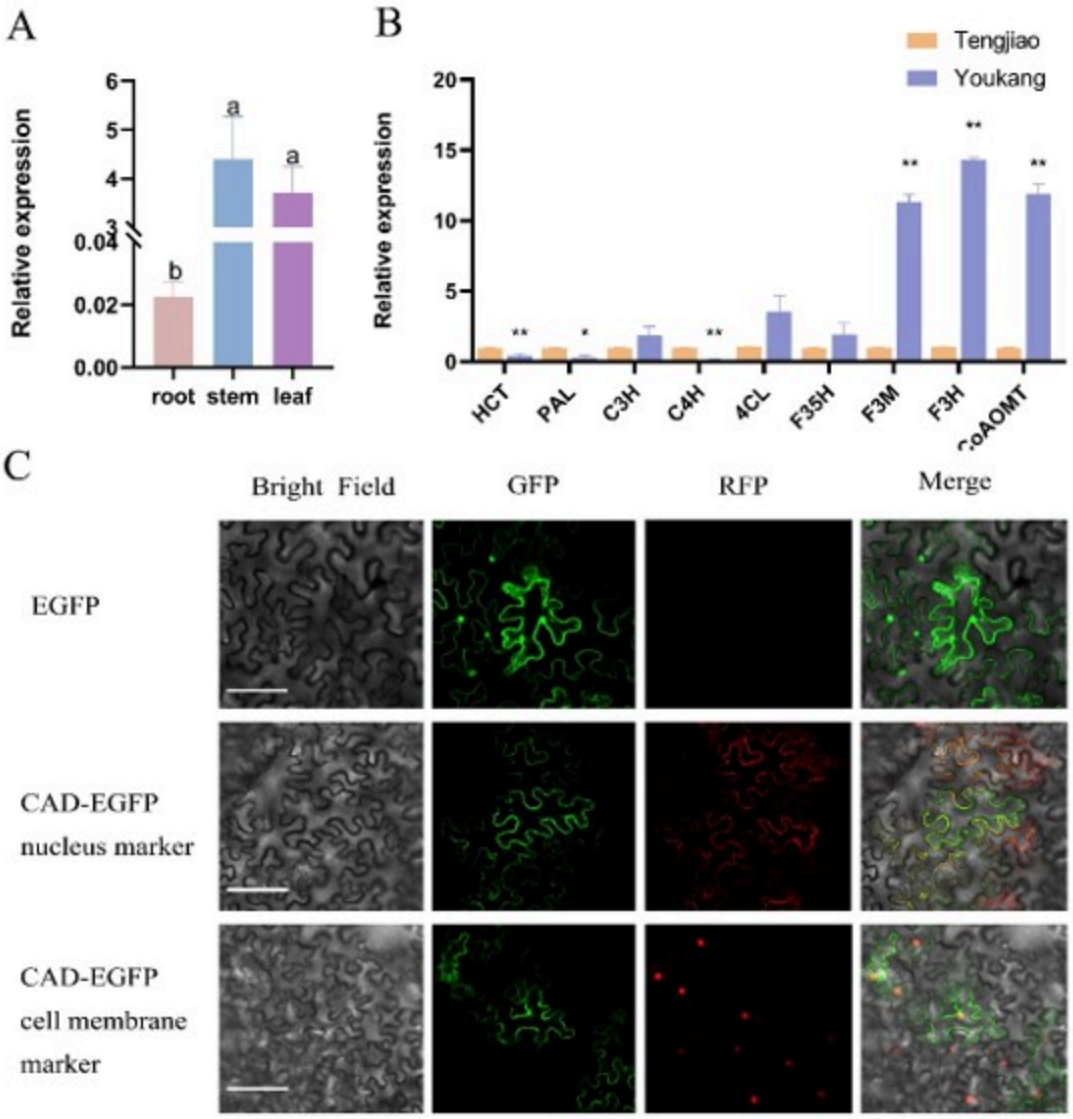

Figure 2

Gene expression analysis and subcellular localization. (A) The expression profile of *ZaCAD* genes in roots, stems, and leaves. (B) Relative expression levels of phenylpropanoid pathway genes (mean ± SE; n=3) were analyzed. Different lowercase letters indicate significant differences at the $P<0.05$ level in the t-test. (C) Subcellular localization of *ZaCAD* in tobacco epidermal cells.

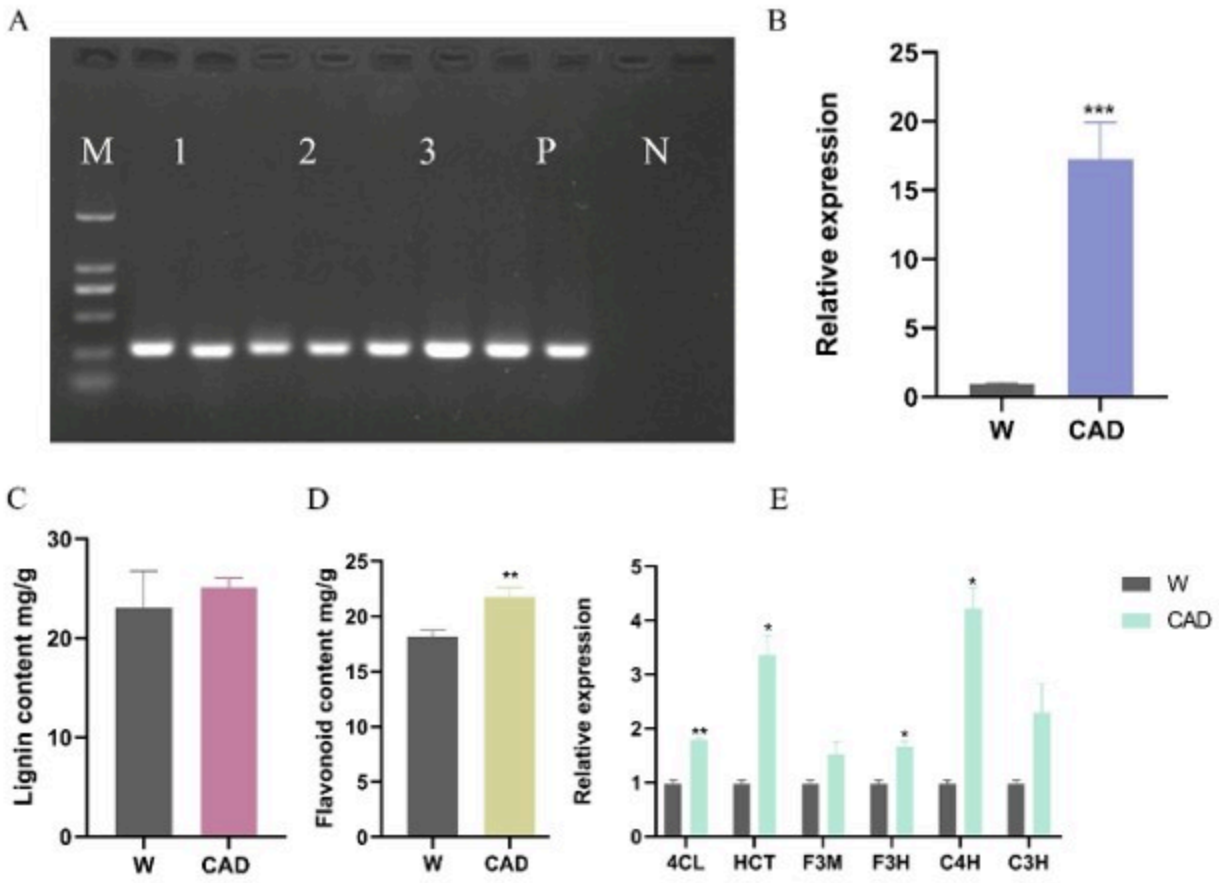

Figure 3

Instantaneous overexpression of *ZaCAD*in *Z. armatum* leaves. (A) Positive transformation strain detection, a total of 3 *ZaCAD* overexpressing lines were obtained. In the electrophoresis map, M represents 2000 markers, and below the numbers 1, 2, and 3, there are two lanes corresponding to two pairs of primer results. P represents the positive control, and N represents the negative control. (B) The relative representation of *ZaCAD* in the processing group. (C) The lignin content in the stem tissue after instantaneous transformation. (D) The total flavonoid content in the stem tissue after instantaneous transformation. (E) The relative expression of phenylpropanoid genes in leaves. All W in the figure are wild-type, and *ZaCAD* represents the processing group. The data is represented as mean ± standard error (n=3); * indicates a significant difference in $P<0.05$ level in t-test, and * * indicates a highly significant difference in $P<0.01$ level in t-test.

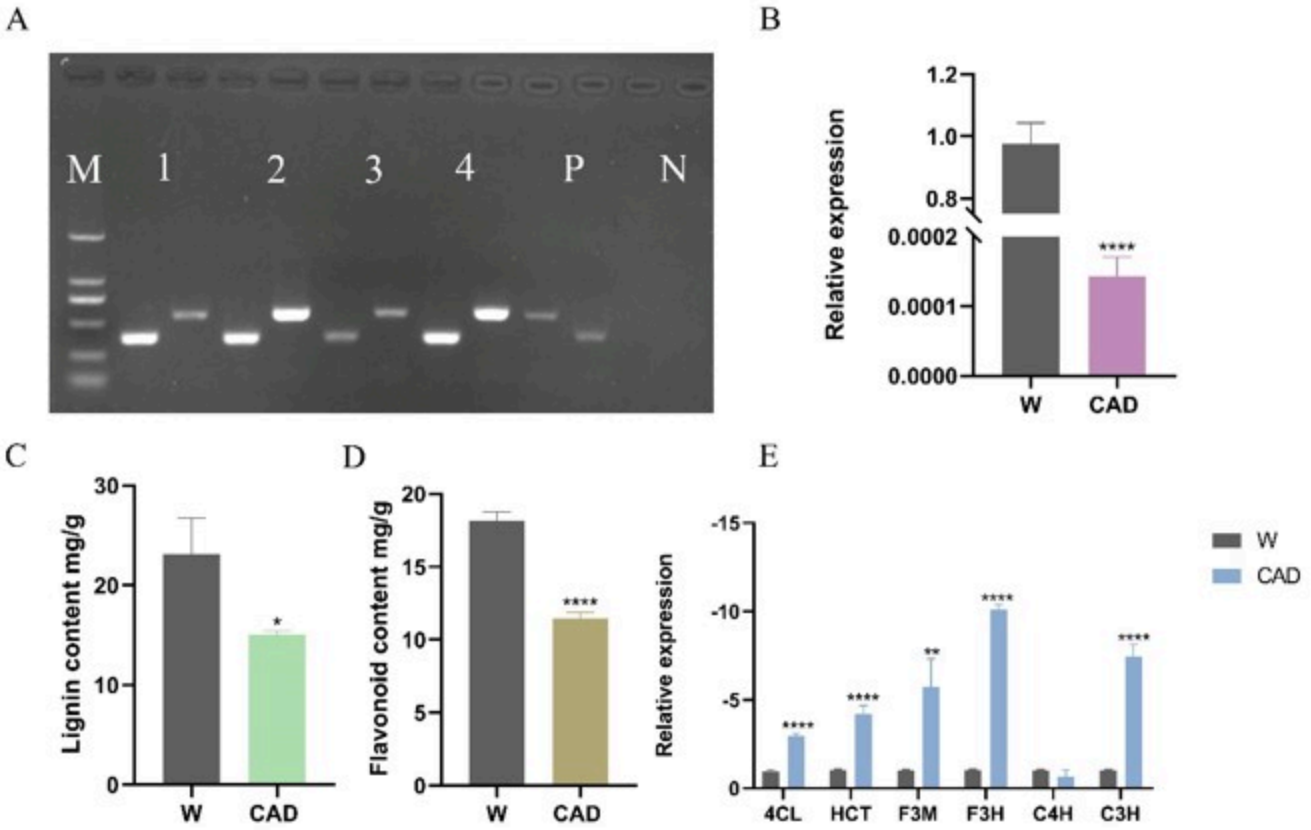

Figure 4

Transient Silence Expression of *ZaCAD*in *Z. armatum* Leaves. (A) Positive transformation strain detection, a total of 4 *ZaCAD* silenced strains were obtained. In the electrophoresis map, M represents 2000marker, and below the numbers 1, 2, 3, and 4, there are two lanes corresponding to two pairs of primer results. P (positive control), N (negative control). (B) The relative expression of *ZaCAD* in blades. (C) The lignin content in the stem tissue after instantaneous transformation. (D) The total flavonoid content in the stem tissue after instantaneous transformation. (E) The relative expression of phenylpropanoid genes in leaves. All W in the figure are wild-type, and *ZaCAD* represents the processing group. The data is represented as mean ± standard error (n=3); **** There is a significant difference in $P<0.05$ level in the t-test.

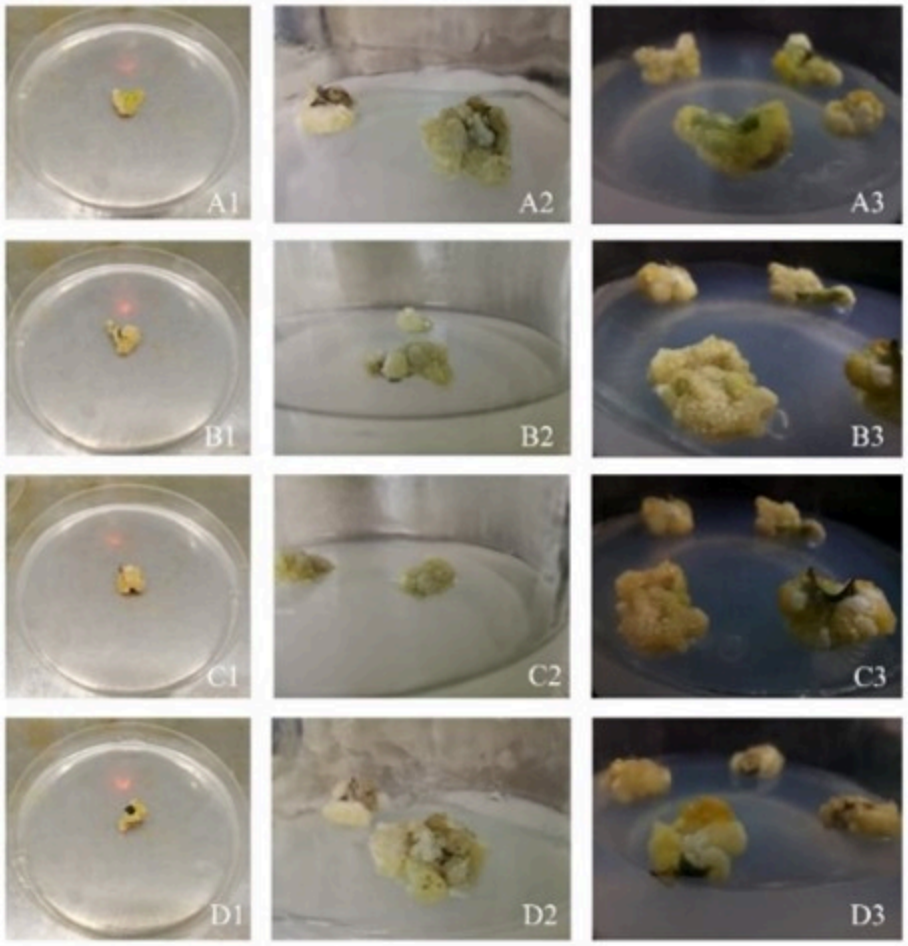

Figure 5

Callus induction and positive screening. (A-D) Group A is the *CAD*-RNAi treatment group, Group B is the *CAD*-overexpression treatment group, Group C is the negative control group, and Group D is the positive control group.

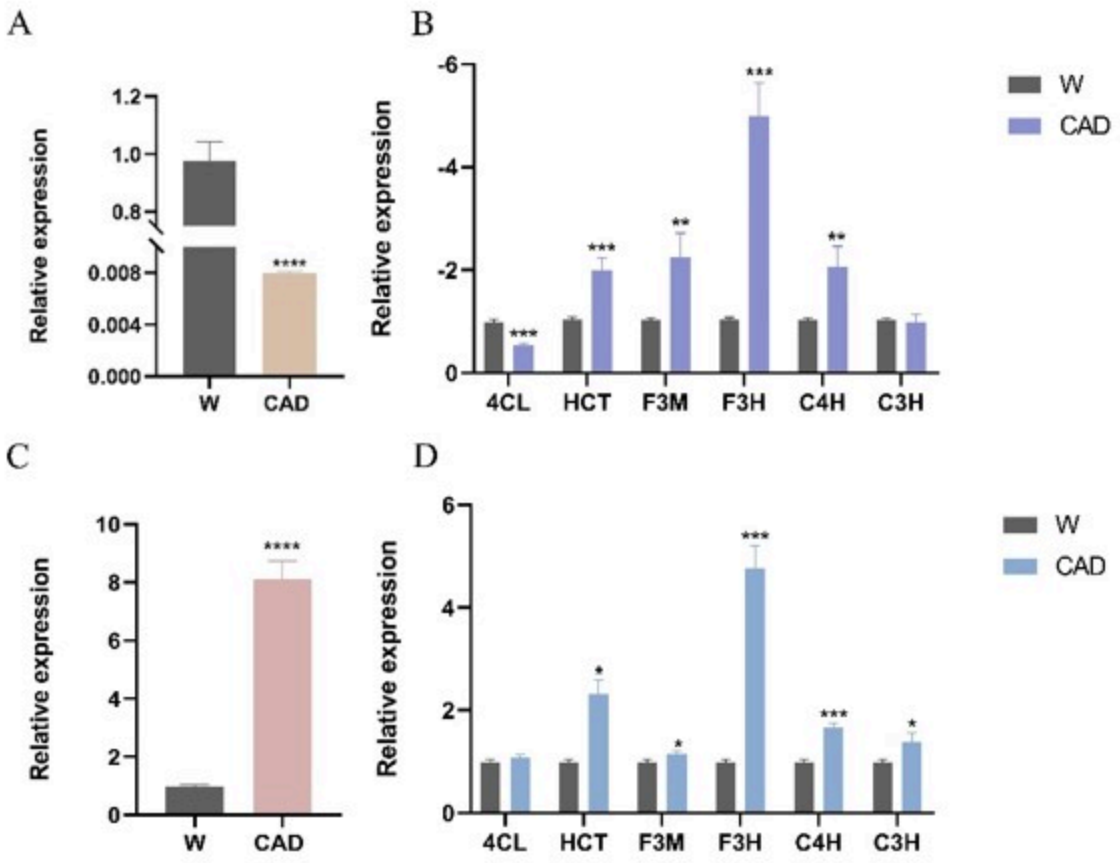

Figure 6

Silent expression and overexpression of *ZaCAD* in *Z. armatum* callus tissue. (A) *Z. armatum* callus induction, A1-A3 is *CAD*-RNAi, B1-B3 is *CAD*-overexpression, C1-C3: positive control, D1-D3: negative control. (B) The relative expression of silent *CAD* in callus tissue. (C) The relative expression of phenylpropanoid related genes in silenced callus tissues. (D) The relative expression of overexpression system *ZaCAD* in callus tissue. (E) The relative expression of phenylpropanoid related genes in overexpressed callus tissues. All W in the figure are wild-type, and *ZaCAD* represents the processing group. The data is represented as mean ± standard error (n=3). **** There is a significant difference in $P<0.05$ level in the t-test.

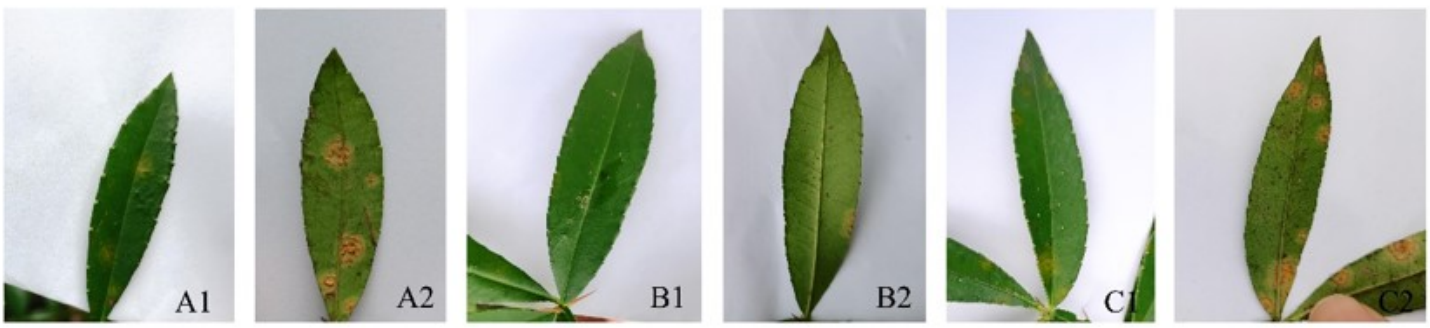

Figure 7

Symptom of rust disease in Chinese pepper induced by artificial inoculation. Group A was the control group, group B was the overexpression treatment group, and group C was the silencing treatment group. The A1, B1, C1 represent the front of the blade, and the A2, B2, C2 represents the back of the blade respectively.

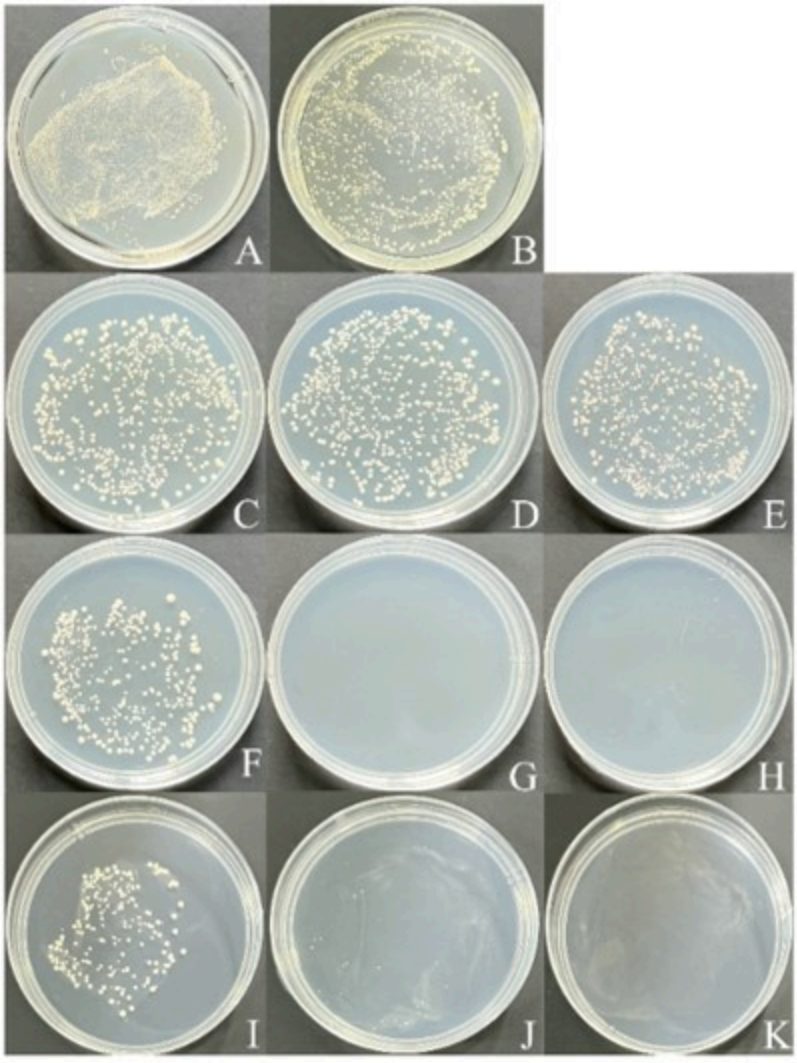

Figure 8

Toxicity and self-activation detection of bait carriers. (A) The colony of pGBKT7 after empty load transformation of yeast. (B) The colony of the recombinant plasmid pGBKT7-*CAD*after being transferred to Y2HGold. (C-E) The diagram shows the co transformation of pGBKT7-53 Control Vector and pGADT7-T Control Vector onto DDO, TDO, and QDO media. (F) The colony shows the co transformation of pGBKT7 Lam Control Vector and pGADT7 T Control Vector into DDO medium. (G) The diagram shows the co transformation of pGBKT7 Lam Control Vector and pGADT7 T Control Vector into TDO medium. (H) The diagram shows the co transformation of pGBKT7 Lam Control Vector and pGADT7 T Control Vector into QDO medium. (I) The colony shows the co transformation of pGBKT7-*CAD* and pGADT7 into DDO medium. (J) The diagram shows the co transformation of pGBKT7-*CAD* and pGADT7 into TDO medium. (K) The diagram shows the co transformation of pGBKT7-*CAD*and pGADT7 into QDO medium.

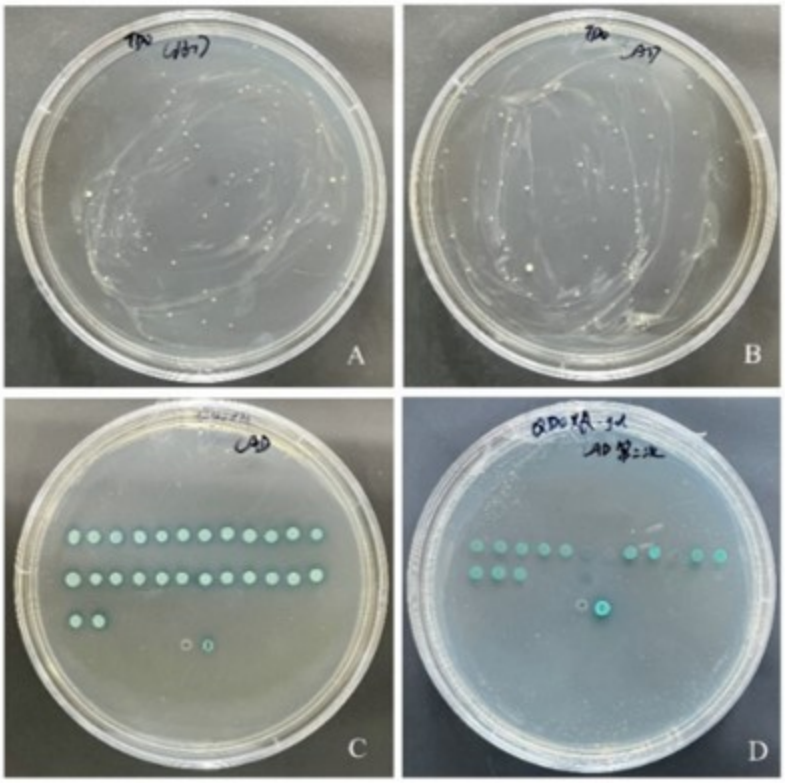

Figure 9

Bait carrier screening library. (A, B) pGBKT7-*ZaCAD* and pGADT7 libraries were co-transformed onto TDO medium for initial screening. (C, D) pGBKT7-*ZaCAD* and pGADT7 libraries co-converted to QDO/AbA/X-α- Perform re screening on Gal medium. +: Positive control, -: Negative control.

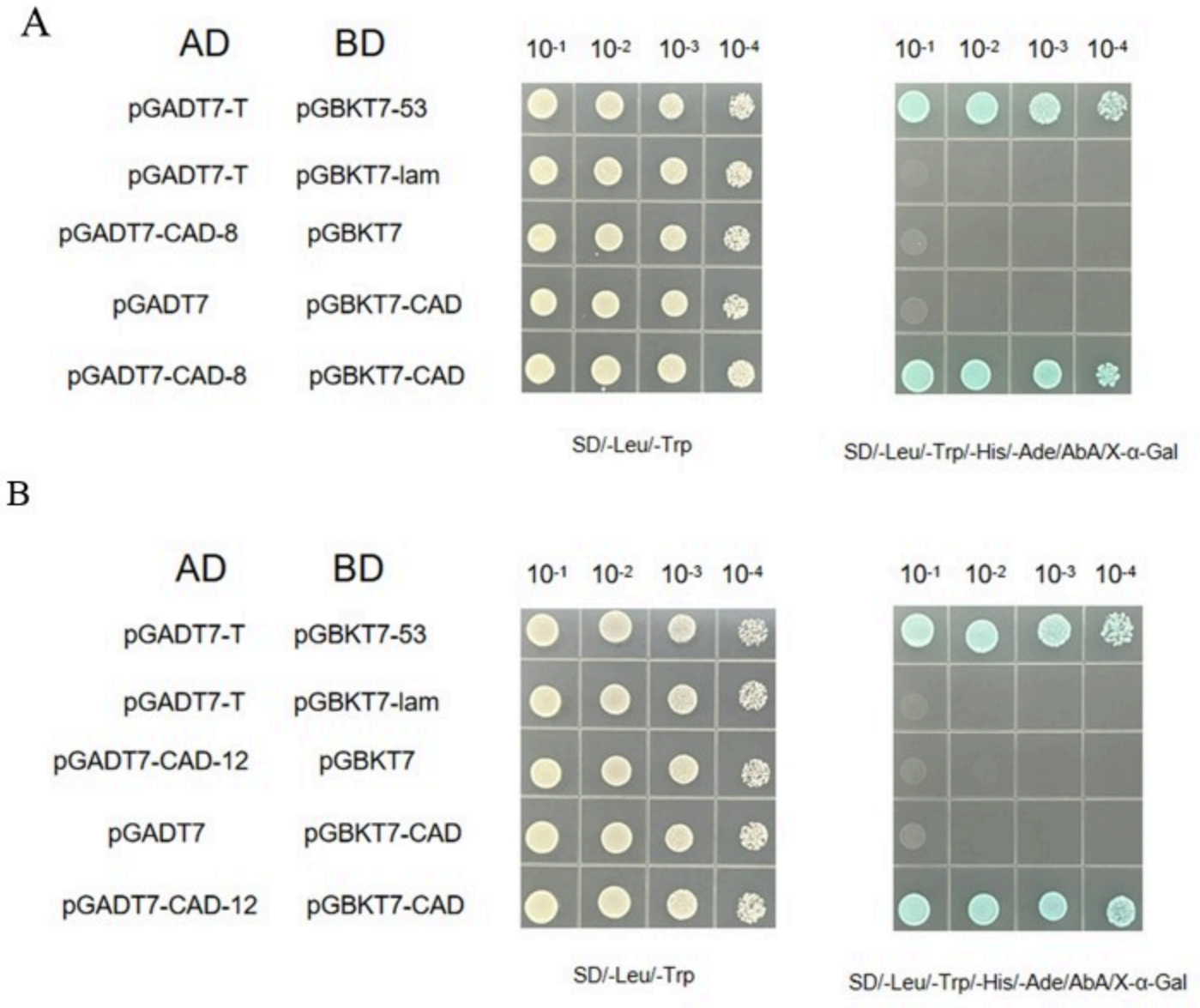

Figure 10

Candidate positive gene gradient dilution point plate verification. (A) pGBKT7-*ZaCAD* and pGADT7-*GAPDH*co-transformed into QDO medium gradient dilution point plate verification. (B) The diagram is pGBKT7-*ZaCAD* and pGADT7-*MDH* co-transformed into a gradient dilution point plate on QDO medium for verification; the pGBKT7-53 Control Vector and pGADT7-T Control Vector were used as positive control. The pGBKT7-Lam Control Vector and pGADT7-T Control Vector were negative controls. The pGBKT7-*ZaCAD* and pGADT7 were empty plasmid control groups.

Supplementary Files

This is a list of supplementary files associated with this preprint. Click to download.

- Appendix1Primerinformationusedinthisarticle.docx